



HAL
open science

PLGA implants for controlled drug release: Impact of the diameter

Celine Bassand, J. Freitag, L. Benabed, Jérémy Verin, Florence Siepmann, Juergen Siepmann

► **To cite this version:**

Celine Bassand, J. Freitag, L. Benabed, Jérémy Verin, Florence Siepmann, et al.. PLGA implants for controlled drug release: Impact of the diameter. *European Journal of Pharmaceutics and Biopharmaceutics*, 2022, *European Journal of Pharmaceutics and Biopharmaceutics*, 177, pp.50-60. 10.1016/j.ejpb.2022.05.020 . hal-04009128

HAL Id: hal-04009128

<https://hal.univ-lille.fr/hal-04009128>

Submitted on 29 Apr 2024

HAL is a multi-disciplinary open access archive for the deposit and dissemination of scientific research documents, whether they are published or not. The documents may come from teaching and research institutions in France or abroad, or from public or private research centers.

L'archive ouverte pluridisciplinaire **HAL**, est destinée au dépôt et à la diffusion de documents scientifiques de niveau recherche, publiés ou non, émanant des établissements d'enseignement et de recherche français ou étrangers, des laboratoires publics ou privés.

Research article

PLGA implants for controlled drug release: Impact of the diameter

C. Bassand, J. Freitag, L. Benabed, J. Verin, F. Siepmann, J. Siepmann*

Univ. Lille, Inserm, CHU Lille, U1008, F-59000 Lille, France

*correspondence:

Prof. Dr. Juergen Siepmann

College of Pharmacy, INSERM U1008

University of Lille

3, rue du Professeur Laguesse

59006 Lille, France

juergen.siepmann@univ-lille.fr

Abstract

The aim of this study was to better understand the importance of the diameter of poly(lactic-co-glycolic acid) (PLGA)-based implants on system performance, in particular the control of drug release. Different types of ibuprofen-loaded implants were prepared by hot melt extrusion using a Leistritz Nano 16 twin-screw extruder. Drug release was measured in well agitated phosphate buffer pH 7.4 bulk fluid and in agarose gels in Eppendorf tubes or transwell plates. Dynamic changes in the implants' dry & wet mass, volume, polymer molecular weight as well as inner & outer morphology were monitored using gravimetric analysis, optical microscopy, gel permeation chromatography and scanning electron microscopy. The physical states of the drug and polymer were determined by DSC. Also pH changes in the release medium were investigated. Irrespective of the type of experimental set-up, the resulting absolute and relative drug release rates decreased with increasing implant diameter (0.7 to 2.8 mm). Bi-phasic drug release was observed in all cases from the monolithic solutions (ibuprofen was dissolved in the polymer): A zero order release phase was followed by a final, rapid drug release phase (accounting for 80-90 % of the total drug dose). The decrease in the relative drug release rate with increasing system diameter can be explained by the increase in the diffusion pathway lengths to be overcome. Interestingly, also the onset of the final rapid drug release phase was delayed with increasing implant diameter. This can probably be attributed to the higher mechanical stability of thicker devices, offering more resistance to substantial entire system swelling.

Keywords: PLGA implant; ibuprofen; swelling; drug release mechanism; monolithic solution

1. Introduction

Poly(lactic-co-glycolic acid) (PLGA) is frequently used as polymeric matrix former to control drug release from implants and microparticles [1–3]. Several PLGA-based, injectable/implantable drug products are available on the market since decades. The reason for the success of this polymer include: (i) its good biocompatibility " [4–6], (ii) complete biodegradability into lactic acid and glycolic acid, and (iii) the possibility to provide desired drug release rates during flexible time periods, ranging from a few hours to several months [7,8]. Alternative biodegradable polymers for parenteral controlled drug delivery include poly(lactic acid), poly(caprolactone) and polyanhydrides [4-6, 9-10]. The choice of the most appropriate biodegradable matrix former for a specific application depends on a variety of factors, including for instance the processability of the material, targeted release period and drug release profile as well as the desired/required mechanical properties of the delivery system, to mention just a few.

Different manufacturing techniques can be used to prepare PLGA-based dosage forms, for example: emulsification – solvent evaporation methods [11,12], compression [13], 3D printing [14] and hot melt extrusion [15–17]. The type of manufacturing method and selected process parameters can significantly affect the resulting inner and outer structure of the dosage forms and, hence, the resulting drug release kinetics [18,19]. Also, the composition of the devices can have a crucial effect, such as the drug loading, type of drug (e.g., its hydrophilicity) [20], type of PLGA (e.g., average polymer molecular weight, type of end groups) [21,22], and potential addition of further excipients [2,23,24]. In this study, hot melt extrusion was chosen, since this technique offers an interesting potential for the preparation of homogeneous drug-polymer blends [16,24,25]. However, care must be taken not to thermally degrade the polymer, nor the drug.

The mass transport mechanisms controlling drug release from a PLGA-based dosage form can be complex [26,27]. Upon contact with aqueous media (e.g. living tissue or phosphate buffer in vitro), water penetrates into the system. This process is generally relatively rapid, assuring that the entire device is wetted and hydrolytic polymer chain cleavage occurs throughout the dosage form (“bulk erosion”) [28,29]. However, initially, the PLGA is rather hydrophobic (in most cases) and the amounts of water inside the system are limited. Importantly, once an ester bond is hydrolyzed, a new -OH and a new -COOH end group are generated. Consequently, the polymeric matrix becomes more and more hydrophilic with time. In addition, the degree of polymer chain entanglement decreases and the matrix becomes mechanically less stable. Furthermore, water-soluble degradation products create a steadily increasing osmotic pressure in the system. This can result in substantial system swelling [30–33]. The presence of pores as well as pore closure [34–36], drug dissolution and diffusion [26,37], the creation of local acidic microenvironments and related autocatalytic effects [38,39], as well as “drug – polymer” and “water – polymer” interactions [40–42] can also play a major role. The relative importance of these phenomena might strongly depend on the type of system, e.g. geometry, size, composition and manufacturing method. Often, it is not fully understood which are the dominant mass transport steps, resulting in sometimes surprising effects of formulation and processing parameters. Hence, the optimization of this type of advanced drug delivery systems can be highly cumbersome, requiring cost-intensive and time-consuming series of trial-and-error experiments.

One of the key properties of a controlled drug delivery system, which can often relatively easily be varied and which might offer the possibility to adjust desired drug release profiles, is the system size [43–46]. This is for example the case, if diffusion plays an important role: Varying the system size means varying the length of the diffusion pathways and, thus, the resulting release rate. However, in the case of initially non-porous PLGA-based microparticles

loaded with small amounts of lidocaine, an increase in system size by a factor of 7 did hardly alter drug release [47]. This could be explained by the increasing importance of autocatalytic effects inside the microparticles: Not only the diffusion pathways for the drug, but also for the generated short chain acids increases with increasing system size. In that study, this effect led to more pronounced drops in the micro pH inside the microparticles and, thus, accelerated polymer degradation (hydrolytic ester bond cleavage is catalyzed by protons) and increased drug mobility: Larger microparticle became much more porous than smaller microparticles during drug release. In contrast, these effects were less pronounced in microparticles based on the same polymer and drug, but which were highly porous from the beginning [48]. In that case, acids and bases were more mobile and pH drops less pronounced. Other parameters, which can be varied to adjust desired drug release patterns from PLGA-based delivery systems include for example the average polymer molecular weight, type of end groups (free acids versus esters), “lactic acid : glycolic acid” ratio, drug loading, addition of further excipients and manufacturing procedure [49-51].

The aim of this study was to better understand the importance of the diameter of PLGA-based implants prepared by hot melt extrusion on ibuprofen release. Differently sized implants were exposed to phosphate buffer pH 7.4 in 3 experimental set-ups: in well agitated bulk fluid, in agarose gels exposed to phosphate buffer in Eppendorf tubes and in agarose gels exposed to phosphate buffer in transwell plates. The gels were intended to mimic living tissue more realistically than bulk fluids [15]. Optical microscopy, gravimetric analysis, DSC, GPC, scanning electron microscopy, and pH measurements were used to monitor the implants' key properties before and after exposure to the release medium.

2. Materials and methods

2.1. Materials

Poly (D,L lactic-co-glycolic acid) (PLGA, 50:50 lactic acid: glycolic acid; Resomer RG 503H; Evonik, Darmstadt, Germany); ibuprofen (BASF, Ludwigshafen, Germany); agarose (genetic analysis grade) and tetrahydrofuran (HPLC grade) (Fisher Scientific, Illkirch, France); potassium dihydrogen orthophosphate and sodium hydroxide (Acros Organics, Geel, Belgium); acetonitrile (VWR, Fontenay-sous-Bois, France); sodium hydrogen phosphate (Na_2HPO_4 ; Panreac Quimica, Barcelona, Spain).

2.2. Implant preparation

PLGA was milled for 4 x 30 s in a grinder (Valentin, Seb, Ecully, France). Appropriate amounts of polymer and drug powders were blended for 5 min with a mortar and a pestle, followed by extrusion using a Nano 16 twin-screw extruder (die diameter = 0.5, 1, 2 or 3 mm, screw diameter = 16 mm, length/diameter ratio = 26.25, gravitational feeder) (Leistritz, Nuremberg, Germany). The process temperatures were kept constant at 80 - 75 - 70 - 65 °C (die - zone 3 - zone 2 - zone 1). The screw speed was set at 50 rpm, the screw configuration is illustrated in Figure S1. After cooling, the hot melt extrudates were manually cut into cylinders of 5 mm length.

2.3. Optical macroscopy

Pictures of implants before exposure to the release medium were taken using a SZN-6 trinocular stereo zoom microscope (Optika, Ponteranica, Italy), equipped with an optical camera (Optika Vision Lite 2.1 software). The lengths and diameters of the implants were

determined using the ImageJ software (US National Institutes of Health, Bethesda, Maryland, USA).

2.4. Practical drug loading

Implants were dissolved in 5 mL acetonitrile, followed filtration (PVDF syringe filters, 0.45 μm ; Agilent Technologies, Santa Clara, USA) and drug content determination by HPLC-UV analysis using a Thermo Fisher Scientific Ultimate 3000 Series HPLC, equipped with a LPG 3400 SD/RS pump, an auto sampler (WPS-3000 SL) and UV-Vis detector (VWD-3400RS) (Thermo Fisher Scientific, Waltham, USA). A reversed phase column C18 (Gemini 5 μm ; 110 \AA ; 150 x 4.6 mm; Phenomenex, Le Pecq, France) was used. The mobile phase was a mixture of 30 mM Na_2HPO_4 pH 7.0: acetonitrile (60:40, v:v). The detection wavelength was 225 nm, and the flow rate 0.5 mL/min. Ten microliter samples were injected. All experiments were conducted in triplicate. Mean values +/- standard deviations are reported.

2.5. Differential scanning calorimetry (DSC)

DSC thermograms of the raw materials (PLGA and ibuprofen) and implants were recorded using a DCS1 Star System (Mettler Toledo, Greifensee, Switzerland). Approximately 5 mg raw material samples and around 10 mg implant samples were heated in perforated aluminum pans as follows: from -70 to 120 $^{\circ}\text{C}$, cooling to -70 $^{\circ}\text{C}$, re-heating to 120 $^{\circ}\text{C}$ (heating/cooling rate = 10 $^{\circ}\text{C}/\text{min}$). The reported glass temperatures (T_g s) were determined from the 1st heating cycles in the case of implants (the thermal history being of interest), and from the 2nd heating cycle in the case of the raw material (the thermal history not being of interest). All experiments were conducted in triplicate. Mean values +/- standard deviations are reported.

2.6. *In vitro* drug release

Three experimental set-ups were used to measure ibuprofen release from the PLGA implants:

In well agitated bulk fluids

Implants were placed in 5 mL Eppendorf tubes (1 implant per tube), filled with 5 mL phosphate buffer pH 7.4 USP 42 (Figure 1A). Metal baskets avoided that the implants sank to the bottom of the tubes (resulting in potentially limited contact with the bulk fluid). The mesh size (250 μm) was sufficient to allow for convective flow and rapid medium exchange “inside – outside” the basket. The tubes were placed in a horizontal shaker (80 rpm, 37°C; GFL 3033; Gesellschaft fuer Labortechnik, Burgwedel, Germany). At predetermined time points, the entire bulk fluid was withdrawn and its volume was measured (to take potential losses due to substantial implant swelling into account). 5 mL pre-heated, fresh phosphate buffer pH 7.4 was added to the tubes. The withdrawn samples were filtered (PVDF syringe filter, 0.45 μm ; Agilent, Santa Clara, California, USA) and analyzed for their ibuprofen contents by HPLC-UV, as described in *section 2.4*.

In agarose gels in Eppendorf tubes

Implants were embedded into agarose gels in 5 mL Eppendorf tubes, as illustrated in Figure 1B (1 implant per tube). An agarose dispersion (0.5% w:v) in phosphate buffer pH 7.4 (USP 42) was heated to 100 °C under magnetic stirring (250 rpm) until a clear solution was obtained. The latter was cooled to 47°C and continuously stirred (to prevent gelation). 0.5 mL of the solution was placed into the bottom of an Eppendorf tube and cooled in a refrigerator for 5 min to allow for gelation. An implant was carefully placed on top of the gel, and covered with a second layer of 0.5 mL agarose solution (47 °C), followed by cooling in a refrigerator for 5 min. Four mL phosphate buffer pH 7.4 USP 42 were added on top of the gel, and the tubes were placed in a horizontal shaker (80 rpm, 37°C; GFL 3033). At predetermined time points,

the bulk fluid was withdrawn, replaced, filtered and analyzed as for the drug release measurements in well agitated bulk fluids.

In agarose gels in transwell plates

Implants were embedded in agarose gels in transwell plates (1 implant per insert, membranes: 1.13 cm², 11 μm, 0.4 μm pore size; Nunc, Roskilde, Denmark), as illustrated in Figure 1C. The agarose gels were prepared as described above, and the implants included accordingly (placed between 2 “layers” of 0.5 mL gel). The well plates were filled with 4 mL phosphate buffer pH 7.4, covered with lids and Parafilm to minimize evaporation, and placed in a horizontal shaker (80 rpm, 37°C; GFL 3033). At predetermined time points, the bulk fluid was withdrawn, replaced, filtered and analyzed as for the drug release measurements in well agitated bulk fluids.

In all cases, sink conditions were provided throughout the experiments in the well-agitated bulk fluids. For each individual implant, the experimentally observed plateau value at the end of the observation period was considered as 100% reference value (the implants completely disappeared, no remnants remained). The measured values were in good agreement with the experimentally determined drug loadings (please see section 2.4 *Practical drug loading*). Furthermore, the pH of the bulk fluids was measured at pre-determined time points using a pH meter (InoLab pH Level 1; WTW, Weilheim, Germany). All experiments were conducted in triplicate. Mean values +/- standard deviations are reported.

2.7. Implant swelling

Implants were treated as for the in vitro drug release studies described in *section 2.6*. At pre-determined time points:

- (i) Pictures of the implants were taken with a SZN-6 trinocular stereo zoom microscope (Optika), equipped with an optical camera (Optika Vision Lite 2.1 software). The

lengths and diameters of the implants were determined using the ImageJ software (US National Institutes of Health). Dynamic changes in the systems' volume were calculated considering cylindrical geometry. At later time points, when the implants were no more perfectly cylindrical in shape, *average* lengths and diameters were estimated. The deviation from cylindrical geometry introduced some error (and increased standard deviations), but the observed tendencies were very clear.

- (ii) Implant samples were withdrawn and excess water was carefully removed using Kimtech precision wipes (Kimberly-Clark, Rouen, France) and weighed (XS105 DualRange balance, 0.01mg readability; Mettler-Toledo, Greifensee, Switzerland) [*wet mass (t)*]. The *change in wet mass (%) (t)* was calculated as follows:

$$\text{change in wet mass } (\%)(t) = \frac{\text{wet mass } (t) - \text{mass } (t=0)}{\text{mass } (t=0)} \times 100 \% \quad (1)$$

where *mass (t = 0)* denotes the implant mass before exposure to the release medium.

All experiments were conducted in triplicate. Mean values +/- standard deviations are reported.

2.8. Implant erosion and PLGA degradation

Implants were treated as for the in vitro drug release studies described in *section 2.6*. At pre-determined time points, implant samples were withdrawn and freeze-dried (freezing at -45°C for 2 h 35 min, primary drying at -20 °C/0.940 mbar for 35 h 10 min and secondary drying at +20 °C/0.0050 mbar for 35 h; Christ Alpha 2-4 LSC+; Martin Christ, Osterode, Germany).

The *dry mass (%) (t)* was calculated as follows:

$$\text{dry mass } (\%)(t) = \frac{\text{dry mass } (t)}{\text{mass } (t=0)} \times 100 \% \quad (2)$$

where $mass(t = 0)$ denotes the implant's mass before exposure to the release medium. All experiments were conducted in triplicate. Mean values +/- standard deviations are reported.

The average polymer molecular weight (Mw) of the PLGA was determined by gel permeation chromatography (GPC) as follows: Freeze-dried implant samples were dissolved in tetrahydrofuran (at a concentration of 3 mg/mL). One hundred μ L samples were injected into an Alliance GPC (refractometer detector: 2414 RI, separation module e2695, Empower GPC software; Waters, Milford, USA), equipped with a PLgel 5 μ m MIXED-D column (kept at 35°C, 7.8 \times 300 mm; Agilent). Tetrahydrofuran was the mobile phase (flow rate: 1 mL/min). Polystyrene standards with molecular weights between 1,480 and 70,950 Da (Polymer Laboratories, Varian, Les Ulis, France) were used to prepare the calibration curve. All experiments were conducted in triplicate. Mean values +/- standard deviations are reported.

2.9. Scanning electronic microscopy (SEM)

The internal and external morphology of the implants before and after exposure to the release medium was studied using a JEOL Field Emission Scanning Electron Microscope (JSM-7800F, Japan), equipped with the Aztec 3.3 software (Oxford Instruments, Oxfordshire, England). Samples were fixed with a ribbon carbon double-sided adhesive and covered with a fine chrome layer. In the case of implants which had been exposed to the release medium, the systems were treated as for the in vitro release studies described in *section 2.6*. At predetermined time points, implant samples were withdrawn, optionally cut (for cross sections) using a scalpel and freeze-dried (as described in *section 2.8*).

3. Results

The aim of this study was to better understand the importance of the diameter of PLGA implants on system performance upon exposure to phosphate buffer pH 7.4 using different experimental set-ups, in particular with respect to the resulting drug release kinetics. Cylindrical ibuprofen-loaded implants were prepared by hot melt extrusion using a Leistritz Nano 16 twin-screw extruder, equipped with differently sized dies. Ibuprofen can be used as an anti-inflammatory drug in certain applications, but it can also be considered as low molecular weight, acidic model drug.

3.1. Implants prior to exposure to the release medium

Figure 2 shows optical macroscopy pictures of the implants prepared with dies with a diameter of 0.5, 1, 2 or 3 mm (as indicated). As it can be seen, they had a homogeneous appearance and smooth surface. The diameters of the implants are indicated in Table 1, ranging from 0.7 to 2.8 mm. The practical drug loading was about 12 % and rather homogeneous in all samples. The polymer molecular weight was about 24-26 kDa, which is slightly higher compared to implants of similar composition prepared by hot melt extrusion using a syringe and heating to 105 °C for 3 to 15 min [52]. This difference can probably be explained by the lower temperatures applied in this study during processing (80 - 75 - 70 - 65 °C: die - zone 3 - zone 2 - zone 1, Figure S1). PLGA is partially cut into shorter chains at elevated temperatures [53]. This also explains the slightly higher glass transition temperatures of the implants prepared in this study (around 35-37 °C) compared to the implants of similar composition prepared at via a heat treatment at 105 °C for 3 to 15 min in a syringe (about 33-34 °C) [52].

Importantly, there were no signs of the presence of *crystalline* drug in the implants prepared using the Nano 16 twin-screw extruder: neither in the DSC thermograms (Figure 3), nor in the SEM pictures of surfaces and cross sections (Figure 4). This is in contrast to implants of similar

composition prepared at 105 °C in a syringe, which contained also some crystalline ibuprofen (in addition to *dissolved* drug) [52]. The much more effective mixing of the drug-polymer blend in the Nano 16 twin-screw extruder during processing (compared to the heated syringe) can likely explain this difference: Convective flow and shear forces facilitate drug dissolution into the PLGA matrix. Figure 3A shows the DSC thermograms of the investigated implants, differing in their diameter. For reasons of comparison, also the thermograms of the PLGA and ibuprofen raw materials were recorded (Figures 3A and B). Clearly, the PLGA was amorphous, while the ibuprofen raw material showed a sharp melting peak at 79.7 +/- 0.5 °C. Importantly, no sign for ibuprofen melting was visible in any implant, only one single glass transition temperature (T_g) could be detected in the investigated temperature range: at about 35-37 °C. The T_g of the PLGA raw material was approximately 47 °C. Thus, ibuprofen clearly acts as a plasticizer for this polymer.

Figure 4 shows SEM pictures of surfaces and cross sections of the differently sized implants before exposure to the release medium. The system diameters are indicated on the left hand-side. As it can be seen, all surfaces and cross sections were smooth and essentially non-porous. Some tiny cavities were visible. As it has previously been demonstrated [52], the ibuprofen can be expected to be essentially dissolved (*molecularly* dispersed) in the polymeric matrix at these drug loadings.

3.2. Implants upon exposure to the release medium

The schemes in Figure 1 shows the 3 experimental set-ups, which were used to monitor drug release from the investigated PLGA implants: (i) Samples were exposed to well agitated phosphate buffer pH 7.4 in Eppendorf tubes (metal baskets with 250 µm meshes assured that the systems did not sink to the bottom of the tubes). (ii) Implants were embedded into agarose gels, which were placed into Eppendorf tubes and exposed to well agitated phosphate buffer

pH 7.4. (iii) Implants were embedded into agarose gels, which were placed into the donor compartments of transwell plates, the acceptor compartments containing well agitated phosphate buffer pH 7.4. The agarose gels were intended to better mimic the conditions upon subcutaneous administration [15]. The top row in Figure 5 shows the *relative* drug release rates from the differently sized PLGA implants observed in the 3 set-ups. Clearly, in all cases, an increase in the implant diameter led to slower relative ibuprofen release. But please note that the opposite trend was observed when looking at the respective *absolute* drug release rates (bottom row in Figure 5). Normalizing the absolute ibuprofen release to the available surface area leads to about similar release rates at the beginning. This is sound, because the drug and polymer are the same, and the composition as well as the inner and outer system structures are very similar (Table 1, Figures 2-4). However, the systems differ substantially in their *total absolute* drug loadings and maximum length of the diffusion pathways to be overcome by the drug. This is why smaller implants were much more rapidly depleted of ibuprofen compared to larger implants (e.g. bottom row in Figure 5).

As it can be seen in Figure 5, the observed drug release kinetics were bi-phasic in all cases, irrespective of the implants' diameter and experimental set-up: An about zero order drug release phase (with an about constant release rate) was followed by a final rapid drug release phase (accounting for approximately 80-90 % of the total drug dose). An initial burst phase was (if present at all) not of noteworthy importance. This is in good agreement with the hypothesis that the initial (limited) burst release (about 3-5 % in the first 12 h) from implants of similar composition, but in which the drug was partially present in the form of crystalline particles, can mainly be attributed to the presence of pure drug particles with direct surface access [52].

Interestingly, all implants did not substantially swell during the first few days after exposure to the release medium, but substantial system swelling set on after a certain lag time : The diagrams in the 2nd row in Figure 5 illustrate the dynamic changes in the implants' volume

as a function of time, Figure 6 shows optical macroscopy pictures of implants studied in the different set-ups at pre-determined time points (please note that upon exposure to well agitated bulk fluids, the samples became too fragile to be withdrawn from the medium after 8 or 10 d). The diagrams in the 2nd row in Figure 7 illustrate the dynamic changes in the implants' wet mass (the top row in this figure shows a zoom on drug release during the first 10 d). Looking at Figures 5 and 7, it becomes obvious that substantial implant swelling and the onset of the final rapid drug release phase coincided in all cases, irrespective of the implants' size and experimental set-up. Furthermore, this onset was delayed when embedding the implants in agarose gels and when increasing the implants' diameter.

These phenomena can probably be explained as follows: Upon contact with aqueous media, limited amounts of water penetrate into the implants, which become rapidly *entirely* wetted. Thus, hydrolytic polymer chain cleavage occurs *throughout* the systems and starts from the beginning ("bulk erosion"). This is also consistent with the observed decrease in the average polymer molecular weight, measured by GPC (bottom row in Figure 7). However, most of the PLGA matrix remains dense (PLGA being hydrophobic, limiting the amounts of water within the systems) and the ibuprofen molecules are effectively trapped. Only surface-near regions undergo substantial swelling: Figure 8 shows SEM pictures of surfaces and cross sections of the investigated PLGA implants after 2, 4 and 8 d exposure to the release media. Please note that the samples had to be dried before SEM analysis, thus, artefacts have been created. The highly wizened structures which can be seen on all surfaces result from the drying of highly swollen PLGA surface layers. Since the polymer at the surface is in contact with very high amounts of water from the beginning, ester bond cleavage is particularly rapid in these zones. Upon cleavage of an ester bond, a new hydrophilic -OH and a new hydrophilic -COOH group are created. This renders the degrading polymer more and more water-loving. In addition, the mechanical stability of the 3-dimensional polymer network decreases (since the

macromolecules become shorter and less entangled, Figure 7 bottom row). Furthermore, water-soluble short chain acids accumulate and create a continuously increasing osmotic pressure. This leads to substantial PLGA swelling once the polymer is sufficiently hydrophilic and the matrix becomes mechanically instable. Importantly, this phenomenon is initially limited to surface-near regions, as it can be seen in the cross sections in Figure 8. With time these highly swollen PLGA surface layer increases in thickness. Importantly, the mobility of ibuprofen molecules located in these regions fundamentally changes: They can be expected to be poorly mobile in the dense, non-swollen PLGA, but to be much more mobile in a highly swollen PLGA gel: The distances between the macromolecules has considerably increased and the polymer chains themselves are much more mobile. This can be expected to result in relatively rapid drug release from highly swollen PLGA zones. Since the rate at which the thickness of the highly swollen surface layer increases can be expected to be about constant (the conditions for the swelling of “deeper” polymer layers do not change over time), also the resulting drug release rate can be expected to be about constant. This is in good agreement with the observed zero order release phases (Figure 5, top row).

This *local*, surface-near PLGA swelling has to be distinguished from the observed substantial entire system swelling occurring after about 5-10 d: Due to the fact that the entire implants are rather rapidly wetted upon contact with the release medium, polymer chain degradation occurs *throughout* the systems (even if at a lower rate compared to the outmost, highly swollen surface layers). Hence, after a certain lag time, the entire implant is sufficiently hydrophilic and mechanically instable and exhibits an osmotic pressure, which attracts *substantial* amounts of water into the *entire* device. This is the onset of fundamental entire system swelling. The consequences for ibuprofen release are the same: It becomes much more mobile in the highly swollen PLGA gel. The optical macroscopic pictures in Figure 6 are consistent with this hypothesis: For example, the mobility of an ibuprofen molecule in the

initially dense PLGA matrix in an implant with an initial diameter of 2.8 mm exposed to a well agitated bulk fluid (top rows) can be expected to be limited during the first few days. However, after about 1 week, the implant tremendously swells and ibuprofen can much more easily be released. But not only the mobility of the *drug* molecules/ions fundamentally increases following substantial system swelling: also the water-soluble degradation products of the PLGA can more easily diffuse out into the surrounding environment. This causes a drop in the pH of the respective bulk fluid (3rd row in Figure 5). Please note that the importance of the observed pH drop can in part also be attributed to the longer sampling period (3 d week end), resulting in short chain accumulation in the bulk fluid. As it can be seen, the drop in pH is more pronounced with larger implants, which can be explained by the higher amounts of PLGA in these systems and, thus, higher amounts of degradation products. The facilitated release of drug and short chain acids in the highly swollen PLGA matrices also leads to the onset of implant erosion, as illustrated in the 3rd row in Figure 7. Before, the dry mass loss is limited, because the polymer matrix is dense and poorly permeable.

When looking at the blue, orange, yellow and green curves in the top row of Figure 5, it can be seen that the onset of the final rapid drug release phase is more and more delayed when the implant diameter increases, irrespective of the experimental set-up. This can be explained by the delayed onset of substantial system swelling (increase in volume in Figure 5, optical macroscopy pictures in Figure 6, increase in wet mass in Figure 7, SEM pictures in Figure 8): Larger matrices can be expected to be mechanically more stable than smaller ones, the mass of the investigated implants varying by a factor of about 20 (Table 1). Interestingly, no signs for the occurrence of important autocatalytic effects were observed in this study during the first 10 d (Figure 7, bottom row), despite the system dimensions. This might eventually be explained by the relatively rapidly occurring substantial *entire* system swelling, which sets on after only about 5 to 10 d (Figures 5-8). Once the PLGA is highly swollen, generated water-soluble acids

can rather rapidly diffuse out and be neutralized, and bases from the release medium can rather rapidly diffuse into the system.

Please note that the green curves in the bottom row of Figure 7 indicate that the polymer molecular weight of the PLGA decreases somewhat slower in the case of implants with an initial diameter of 2.8 mm, in contrast to all other implants, which showed very similar polymer degradation kinetics in the observation period. This might eventually indicate that the water content, especially at the center of the implants, might be lower for this largest type of implants. Also the SEM pictures of cross-sections obtained after exposure to the release medium might indicate a structure which is different at the systems' center in the case of the 2.8 mm implants (Figure 8).

Comparing the implant swelling kinetics in the 3 experimental set-ups in Figure 5 (increase in volume), Figure 6 (optical macroscopy), Figure 7 (increase in wet mass) and Figure 8 (SEM pictures), it can be seen that the presence of the agarose gel surrounding the implants delays substantial device swelling. This is probably due to the steric hindrance caused by the gels. As a consequence, also the onset of the final rapid drug release phase is delayed in the gel set-ups (Figure 5, top row), as well as the onset of implant erosion (Figure 7, 3rd row) and of the drop in the pH of the bulk fluid (Figure 5, 3rd row). In vitro release set-ups in which the implants are embedded within a hydrogel are likely better mimicking the conditions encountered in vivo. However, in practice the presence of a gel renders the experiment more cumbersome. When straightforward bulk fluid set-ups are used for reasons of simplicity, the missing impact of the presence of surrounding tissue (e.g., affecting device swelling) should not be forgotten.

4. Conclusions

The variation of the diameter of a PLGA implant is an effective tool to adjust desired absolute and relative release kinetics. In the case of hot melt extruded ibuprofen-loaded implants, bi-phasic release patterns were observed: A zero order release phase was followed by a rapid, final drug release phase (accounting for 80-90 % of the total drug dose). The decrease in the *relative* drug release rate with increasing system diameter can be attributed to the longer diffusion pathways to be overcome. The onset of the final rapid drug release phase was delayed, because the larger polymer matrices are mechanically more stable, retarding the onset of substantial entire implant swelling, which facilitates drug release.

Acknowledgments

This project has received funding from the Interreg 2 Seas programme 2014-2020 co-funded by the European Regional Development Fund under subsidy contract No 2S04-014 3DMed. The Authors would also like to thank Mr. A. Fadel from the “Centre Commun de Microscopie” of the University of Lille (“Plateau technique de la Federation Chevreul CNRS FR 2638”) for his valuable technical help with the SEM pictures.

References

- [1] N.H. Shah, A.S. Railkar, F.C. Chen, R. Tarantino, S. Kumar, M. Murjani, D. Palmer, M.H. Infeld, A.W. Malick, A biodegradable injectable implant for delivering micro and macromolecules using poly (lactic-co-glycolic) acid (PLGA) copolymers, *J. Controlled Release*. 27 (1993) 139–147. [https://doi.org/10.1016/0168-3659\(93\)90217-S](https://doi.org/10.1016/0168-3659(93)90217-S).
- [2] G. Schliecker, C. Schmidt, S. Fuchs, A. Ehinger, J. Sandow, T. Kissel, In vitro and in vivo correlation of busarelin release from biodegradable implants using statistical moment analysis, *J. Control. Release Off. J. Control. Release Soc.* 94 (2004) 25–37. <https://doi.org/10.1016/j.jconrel.2003.09.003>.
- [3] V.B. Kraus, P.G. Conaghan, H.A. Aazami, P. Mehra, A.J. Kivitz, J. Lufkin, J. Hauben, J.R. Johnson, N. Bodick, Synovial and systemic pharmacokinetics (PK) of triamcinolone acetonide (TA) following intra-articular (IA) injection of an extended-release microsphere-based formulation (FX006) or standard crystalline suspension in patients with knee osteoarthritis (OA), *Osteoarthritis Cartilage*. 26 (2018) 34–42. <https://doi.org/10.1016/j.joca.2017.10.003>.
- [4] L.S. Nair, C.T. Laurencin, Biodegradable polymers as biomaterials, *Prog. Polym. Sci.* 32 (2007) 762–798. <https://doi.org/10.1016/j.progpolymsci.2007.05.017>.
- [5] S. Grund, M. Bauer, D. Fischer, Polymers in Drug Delivery—State of the Art and Future Trends, *Adv. Eng. Mater.* 13 (2011) B61–B87. <https://doi.org/10.1002/adem.201080088>.
- [6] J.M. Anderson, M.S. Shive, Biodegradation and biocompatibility of PLA and PLGA microspheres, *Adv. Drug Deliv. Rev.* 64 (2012) 72–82. <https://doi.org/10.1016/j.addr.2012.09.004>.
- [7] V. Schreiner, P. Detampel, P. Jirkof, M. Puchkov, J. Huwyler, Buprenorphine loaded PLGA microparticles: Characterization of a sustained-release formulation, *J. Drug Deliv. Sci. Technol.* 63 (2021) 102558. <https://doi.org/10.1016/j.jddst.2021.102558>.

- [8] M.J. Dorta, A. Santoveña, M. Llabrés, J.B. Fariña, Potential applications of PLGA film-implants in modulating in vitro drugs release, *Int. J. Pharm.* 248 (2002) 149–156. [https://doi.org/10.1016/S0378-5173\(02\)00431-3](https://doi.org/10.1016/S0378-5173(02)00431-3).
- [9] R.S. van der Kooij, R. Steendam, H. W. Frijlink, W.L.J. Hinrichs, An overview of the production methods for core–shell microspheres for parenteral controlled drug delivery, *Eur. J. Pharm. Biopharm.* 170 (2022) 24–42. <https://doi.org/10.1016/j.ejpb.2021.11.007>.
- [10] S.A. Stewart, J. Domínguez-Robles, E. Utomo, C.J. Picco, F. Corduas, E. Mancuso, M. Nur Amir, M. Akbar Bahar, S. Sumarheni, R.F. Donnelly, A. Dian Permana, E. Larraneta, Poly(caprolactone)-based subcutaneous implant for sustained delivery of levothyroxine, *Int. J. Pharmaceut.* 607 (2021) 121011, 1–10. <https://doi.org/10.1016/j.ijpharm.2021.121011>.
- [11] G. Schwach, N. Oudry, S. Delhomme, M. Lück, H. Lindner, R. Gurny, Biodegradable microparticles for sustained release of a new GnRH antagonist – part I: screening commercial PLGA and formulation technologies, *Eur. J. Pharm. Biopharm.* 56 (2003) 327–336. [https://doi.org/10.1016/S0939-6411\(03\)00096-1](https://doi.org/10.1016/S0939-6411(03)00096-1).
- [12] J. Présemy, G. Salzano, G. Courties, M. Shires, F. Ponchel, C. Jorgensen, F. Apparailly, G. De Rosa, PLGA microspheres encapsulating siRNA anti-TNFalpha: Efficient RNAi-mediated treatment of arthritic joints, *Eur. J. Pharm. Biopharm.* 82 (2012) 457–464. <https://doi.org/10.1016/j.ejpb.2012.07.021>.
- [13] M. Takahashi, H. Onishi, Y. Machida, Development of implant tablet for a week-long sustained release, *J. Controlled Release.* 100 (2004) 63–74. <https://doi.org/10.1016/j.jconrel.2004.07.031>.
- [14] T. Guo, C.G. Lim, M. Noshin, J.P. Ringel, J.P. Fisher, 3D printing bioactive PLGA scaffolds using DMSO as a removable solvent, *Bioprinting.* 10 (2018) e00038. <https://doi.org/10.1016/j.bprint.2018.e00038>.

- [15] C. Bassand, J. Verin, M. Lamatsch, F. Siepmann, J. Siepmann, How agarose gels surrounding PLGA implants limit swelling and slow down drug release, *J. Control. Release*, *in press*.
- [16] L. Duque, M. Körber, R. Bodmeier, Improving release completeness from PLGA-based implants for the acid-labile model protein ovalbumin, *Int. J. Pharm.* 538 (2018) 139–146. <https://doi.org/10.1016/j.ijpharm.2018.01.026>.
- [17] M. Goel, D. Leung, A. Famili, D. Chang, P. Nayak, M. Al-Sayah, Accelerated in vitro release testing method for a long-acting peptide-PLGA formulation, *Eur. J. Pharm. Biopharm.* 165 (2021) 185–192. <https://doi.org/10.1016/j.ejpb.2021.05.008>.
- [18] J.V. Andhariya, R. Jog, J. Shen, S. Choi, Y. Wang, Y. Zou, D.J. Burgess, Development of Level A in vitro-in vivo correlations for peptide loaded PLGA microspheres, *J. Control. Release Off. J. Control. Release Soc.* 308 (2019) 1–13. <https://doi.org/10.1016/j.jconrel.2019.07.013>.
- [19] K. Vay, S. Scheler, W. Frieß, Application of Hansen solubility parameters for understanding and prediction of drug distribution in microspheres, *Int. J. Pharm.* 416 (2011) 202–209. <https://doi.org/10.1016/j.ijpharm.2011.06.047>.
- [20] D. Grizić, A. Lamprecht, Predictability of drug encapsulation and release from propylene carbonate/PLGA microparticles, *Int. J. Pharm.* 586 (2020) 119601. <https://doi.org/10.1016/j.ijpharm.2020.119601>.
- [21] B.S. Zolnik, D.J. Burgess, Evaluation of in vivo–in vitro release of dexamethasone from PLGA microspheres, *J. Controlled Release.* 127 (2008) 137–145. <https://doi.org/10.1016/j.jconrel.2008.01.004>.
- [22] P. Xiao, P. Qi, J. Chen, Z. Song, Y. Wang, H. He, X. Tang, P. Wang, The effect of polymer blends on initial release regulation and in vitro-in vivo relationship of peptides loaded

- PLGA-Hydrogel Microspheres, *Int. J. Pharm.* 591 (2020) 119964.
<https://doi.org/10.1016/j.ijpharm.2020.119964>.
- [23] S. Thalhauser, D. Peterhoff, R. Wagner, M. Breunig, Silica particles incorporated into PLGA-based in situ-forming implants exploit the dual advantage of sustained release and particulate delivery, *Eur. J. Pharm. Biopharm.* 156 (2020) 1–10.
<https://doi.org/10.1016/j.ejpb.2020.08.020>.
- [24] E. Lehner, D. Gündel, A. Liebau, S. Plontke, K. Mäder, Intracochlear PLGA based implants for dexamethasone release: Challenges and solutions, *Int. J. Pharm.* X. 1 (2019) 100015. <https://doi.org/10.1016/j.ijpx.2019.100015>.
- [25] J. Breitenbach, Melt extrusion: from process to drug delivery technology, *Eur. J. Pharm. Biopharm.* 54 (2002) 107–117. [https://doi.org/10.1016/S0939-6411\(02\)00061-9](https://doi.org/10.1016/S0939-6411(02)00061-9).
- [26] S.S. Shah, Y. Cha, C.G. Pitt, Poly (glycolic acid-co-dl-lactic acid): diffusion or degradation controlled drug delivery?, *J. Controlled Release.* 18 (1992) 261–270.
[https://doi.org/10.1016/0168-3659\(92\)90171-M](https://doi.org/10.1016/0168-3659(92)90171-M).
- [27] S. Fredenberg, M. Wahlgren, M. Reslow, A. Axelsson, The mechanisms of drug release in poly(lactic-co-glycolic acid)-based drug delivery systems—A review, *Int. J. Pharm.* 415 (2011) 34–52. <https://doi.org/10.1016/j.ijpharm.2011.05.049>.
- [28] A. Göpferich, Mechanisms of polymer degradation and erosion, *Biomaterials.* 17 (1996) 103–114. [https://doi.org/10.1016/0142-9612\(96\)85755-3](https://doi.org/10.1016/0142-9612(96)85755-3).
- [29] F. von Burkersroda, L. Schedl, A. Göpferich, Why degradable polymers undergo surface erosion or bulk erosion, *Biomaterials.* 23 (2002) 4221–4231.
[https://doi.org/10.1016/S0142-9612\(02\)00170-9](https://doi.org/10.1016/S0142-9612(02)00170-9).
- [30] H. Gasmi, F. Danede, J. Siepmann, F. Siepmann, Does PLGA microparticle swelling control drug release? New insight based on single particle swelling studies, *J. Controlled Release.* 213 (2015) 120–127. <https://doi.org/10.1016/j.jconrel.2015.06.039>.

- [31] F. Tamani, C. Bassand, M.C. Hamoudi, F. Danede, J.F. Willart, F. Siepmann, J. Siepmann, Mechanistic explanation of the (up to) 3 release phases of PLGA microparticles: Diprophylline dispersions, *Int. J. Pharm.* 572 (2019) 118819. <https://doi.org/10.1016/j.ijpharm.2019.118819>.
- [32] C. Bode, H. Kranz, A. Fizez, F. Siepmann, J. Siepmann, Often neglected: PLGA/PLA swelling orchestrates drug release: HME implants, *J. Control. Release Off. J. Control. Release Soc.* 306 (2019) 97–107. <https://doi.org/10.1016/j.jconrel.2019.05.039>.
- [33] B. Gu, X. Sun, F. Papadimitrakopoulos, D.J. Burgess, Seeing is believing, PLGA microsphere degradation revealed in PLGA microsphere/PVA hydrogel composites, *J. Controlled Release.* 228 (2016) 170–178. <https://doi.org/10.1016/j.jconrel.2016.03.011>.
- [34] H.K. Kim, H.J. Chung, T.G. Park, Biodegradable polymeric microspheres with “open/closed” pores for sustained release of human growth hormone, *J. Controlled Release.* 112 (2006) 167–174. <https://doi.org/10.1016/j.jconrel.2006.02.004>.
- [35] T. Wang, P. Xue, A. Wang, M. Yin, J. Han, S. Tang, R. Liang, Pore change during degradation of octreotide acetate-loaded PLGA microspheres: The effect of polymer blends, *Eur. J. Pharm. Sci.* 138 (2019) 104990. <https://doi.org/10.1016/j.ejps.2019.104990>.
- [36] N.P. Tipnis, J. Shen, D. Jackson, D. Leblanc, D.J. Burgess, Flow-through cell-based in vitro release method for triamcinolone acetonide poly (lactic-co-glycolic) acid microspheres, *Int. J. Pharm.* 579 (2020) 119130. <https://doi.org/10.1016/j.ijpharm.2020.119130>.
- [37] B.S. Zolnik, P.E. Leary, D.J. Burgess, Elevated temperature accelerated release testing of PLGA microspheres, *J. Control. Release Off. J. Control. Release Soc.* 112 (2006) 293–300. <https://doi.org/10.1016/j.jconrel.2006.02.015>.

- [38] A.G. Ding, A. Shenderova, S.P. Schwendeman, Prediction of Microclimate pH in Poly(lactic-co-glycolic Acid) Films, *J. Am. Chem. Soc.* 128 (2006) 5384–5390. <https://doi.org/10.1021/ja055287k>.
- [39] H. Antheunis, J.-C. van der Meer, M. de Geus, A. Heise, C.E. Koning, Autocatalytic Equation Describing the Change in Molecular Weight during Hydrolytic Degradation of Aliphatic Polyesters, *Biomacromolecules*. 11 (2010) 1118–1124. <https://doi.org/10.1021/bm100125b>.
- [40] P. Blasi, S.S. D'Souza, F. Selmin, P.P. DeLuca, Plasticizing effect of water on poly(lactide-co-glycolide), *J. Controlled Release*. 108 (2005) 1–9. <https://doi.org/10.1016/j.jconrel.2005.07.009>.
- [41] P. Blasi, A. Schoubben, S. Giovagnoli, L. Perioli, M. Ricci, C. Rossi, Ketoprofen poly(lactide-co-glycolide) physical interaction, *AAPS PharmSciTech*. 8 (2007) E78–E85. <https://doi.org/10.1208/pt0802037>.
- [42] C. Zlomke, M. Barth, K. Mäder, Polymer degradation induced drug precipitation in PLGA implants – Why less is sometimes more, *Eur. J. Pharm. Biopharm.* 139 (2019) 142–152. <https://doi.org/10.1016/j.ejpb.2019.03.016>.
- [43] M. Dunne, O.I. Corrigan, Z. Ramtoola, Influence of particle size and dissolution conditions on the degradation properties of polylactide-co-glycolide particles, *Biomaterials*. 21 (2000) 1659–1668. [https://doi.org/10.1016/S0142-9612\(00\)00040-5](https://doi.org/10.1016/S0142-9612(00)00040-5).
- [44] J. Siepmann, N. Faisant, J. Akiki, J. Richard, J.P. Benoit, Effect of the size of biodegradable microparticles on drug release: experiment and theory, *J. Control. Release Off. J. Control. Release Soc.* 96 (2004) 123–134. <https://doi.org/10.1016/j.jconrel.2004.01.011>.

- [45] W. Chen, A. Palazzo, W.E. Hennink, R.J. Kok, Effect of Particle Size on Drug Loading and Release Kinetics of Gefitinib-Loaded PLGA Microspheres, *Mol. Pharm.* 14 (2017) 459–467. <https://doi.org/10.1021/acs.molpharmaceut.6b00896>.
- [46] X. Lin, H. Yang, L. Su, Z. Yang, X. Tang, Effect of size on the in vitro/in vivo drug release and degradation of exenatide-loaded PLGA microspheres, *J. Drug Deliv. Sci. Technol.* 45 (2018) 346–356. <https://doi.org/10.1016/j.jddst.2018.03.024>.
- [47] J. Siepmann, K. Elkharraz, F. Siepmann, D. Klose, How autocatalysis accelerates drug release from PLGA-based microparticles: a quantitative treatment, *Biomacromolecules* 6 (2005) 2312–2319. <https://doi.org/10.1021/bm050228k>.
- [48] D. Klose, F. Siepmann, K. Elkharraz, S. Krenzlin, J. Siepmann, How porosity and size affect the drug release mechanisms from PLGA-based microparticles, *Int. J. Pharm.* 314 (2006) 198–206. <https://doi.org/10.1016/j.ijpharm.2005.07.031>.
- [49] R. Varela-Fernandez, C. Bendicho-Lavilla, F.J. Otero-Espinar, Design, optimization, and in vitro characterization of idebenone-loaded PLGA microspheres for LHON treatment, *Int. J. Pharmaceut.* 616 (2022) 121504, 1-19 <https://doi.org/10.1016/j.ijpharm.2022.121504>.
- [50] P. Maturavongsadit, G. Paravyan, M. Kovarova, J.V. Garcia, S.R. Benhabbour, A new engineering process of biodegradable polymeric solid implants for ultra-long-acting drug delivery, *Int. J. Pharmaceut.* X, 3 (2021) 100068, 1-16. <https://doi.org/10.1016/j.ijpx.2020.100068>.
- [51] C. Zhang, L. Yang, F. Wan, H. Bera, D. Cun, J. Rantanen, M. Yang, Quality by design thinking in the development of long-acting injectable PLGA/PLA-based microspheres for peptide and protein drug delivery, *Int. J. Pharmaceut.* 585 (2020) 119441, 1-19. <https://doi.org/10.1016/j.ijpharm.2020.119441>].

- [52] C. Bassand, L. Benabed, J. Verin, F. Danede, L.A. Lefol, J.F. Willart, F. Siepmann, J. Siepmann, Hot melt extruded PLGA implants loaded with ibuprofen: How heat exposure alters the physical drug state, *J. Drug Deliv. Sci. Technol.* *in press* (2022) <https://doi.org/10.1016/j.jddst.2022.103432>.
- [53] M.L. Houchin, E.M. Topp, Physical properties of PLGA films during polymer degradation, *J. Appl. Polym. Sci.* 114 (2009) 2848–2854. <https://doi.org/10.1002/app.30813>.

Table 1:

Key properties of the investigated ibuprofen-loaded PLGA implants (Tg: glass transition temperature, Mw: average polymer molecular weight). Mean values \pm standard deviations are indicated (n = 3).

Implant	<i>Diameter, die</i>			
	<i>0.5 mm</i>	<i>1 mm</i>	<i>2 mm</i>	<i>3 mm</i>
Diameter (mm)	0.66 \pm 0.02	1.08 \pm 0.02	1.98 \pm 0.03	2.79 \pm 0.19
Weight (mg)	2.53 \pm 0.10	6.84 \pm 0.21	23.58 \pm 1.11	46.22 \pm 6.83
Practical loading (%)	12.1 \pm 0.1	12.5 \pm 0.1	12.3 \pm 0.1	12.0 \pm 0.1
Tg (°C)	35.6 \pm 0.2	35.2 \pm 0.2	36.2 \pm 0.1	36.9 \pm 0.3
Mw (kDa)	23.9 \pm 0.3	24.5 \pm 0.3	25.7 \pm 0.1	24.6 \pm 0.4

Figure captions

Fig 1 Schematic presentations of the experimental set-ups used to monitor drug release from the PLGA-based implants: (A) In well-agitated release medium in Eppendorf tubes (with metal baskets), (B) In agarose gels in Eppendorf tubes, the gels being exposed to well-agitated release medium, (C) In agarose gels in transwell plates, the receptor compartment containing well-agitated release medium. In all cases, sink conditions were provided throughout the experiments in the well-agitated bulk fluids. Details are described in the text.

Fig 2 Optical macroscopy pictures of implants before exposure to release medium. The diameter of the die used for hot melt extrusion is indicated at the top.

Fig 3 DSC thermograms of: (A) PLGA raw material and the investigated ibuprofen-loaded implants (the diameter of the implants are indicated on the left hand-side), and (B) ibuprofen raw material.

Fig 4 Scanning electronic microscopy pictures of surfaces and cross sections of implants before exposure to release medium. The diameters of the implants are indicated on the left hand-side.

Fig 5 Behavior of the ibuprofen-loaded PLGA implants upon exposure to phosphate buffer pH 7.4 using 3 experimental set-ups: Relative (%) and absolute (mg) ibuprofen release kinetics (top and bottom rows), dynamic changes in the implant volume and pH of the well agitated bulk fluids (middle rows). The implant diameters are indicated in the diagrams.

Fig 6 Optical macroscopy pictures ibuprofen-loaded PLGA implants upon exposure to phosphate buffer pH 7.4 in the 3 experimental set-ups: In bulk fluids in Eppendorf tubes, in agarose gels exposed to the release medium in Eppendorf tubes, and in agarose gels in transwell plates containing the release medium in the acceptor compartment. In the

case of the bulk fluids, the implants became too fragile after 8 or 10 d to allow sample withdrawal for imaging.

Fig 7 Zoom on the first 10 d of implant exposure to phosphate buffer pH 7.4 using the 3 experimental set-ups: Relative drug release, dynamic changes in the wet mass & dry mass of the systems and in the average polymer molecular weight of the PLGA. The implant diameters are indicated in the diagrams.

Fig 8 SEM pictures of surfaces and cross sections of ibuprofen-loaded PLGA implants after exposure for 2, 4 or 8 d to phosphate buffer pH 7.4 (as indicated on the left hand-side). Please note that the implants were freeze-dried prior to analysis, creating artefacts. The implant diameters are also indicated in the diagrams. The red and green rectangles indicate specific regions observed at different degrees of magnification.

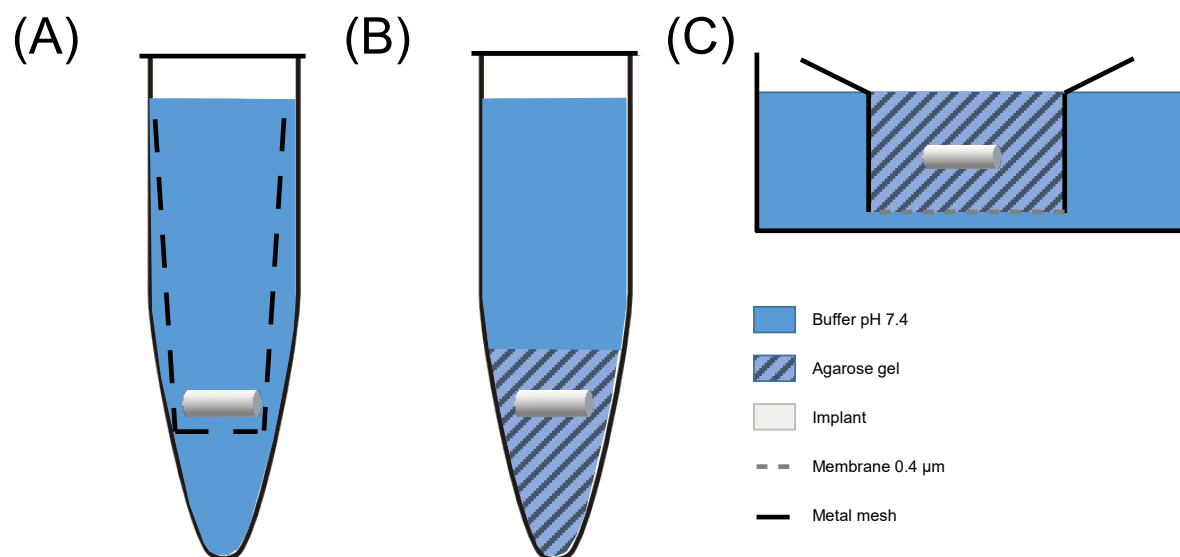


Figure 1

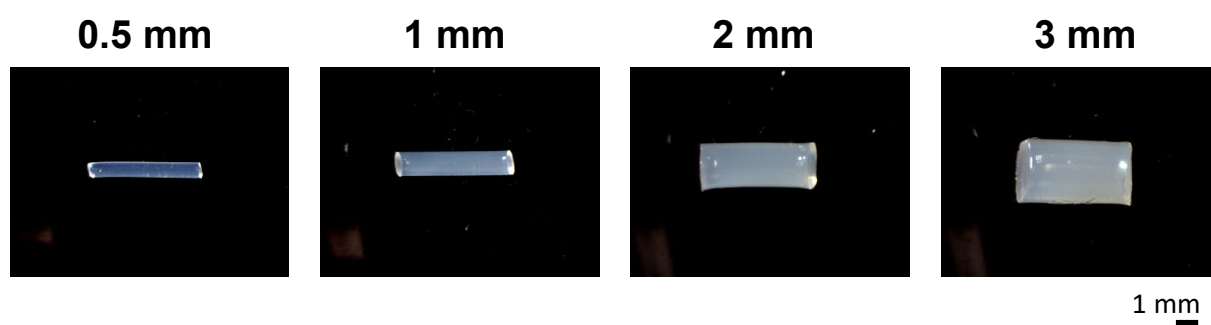


Figure 2

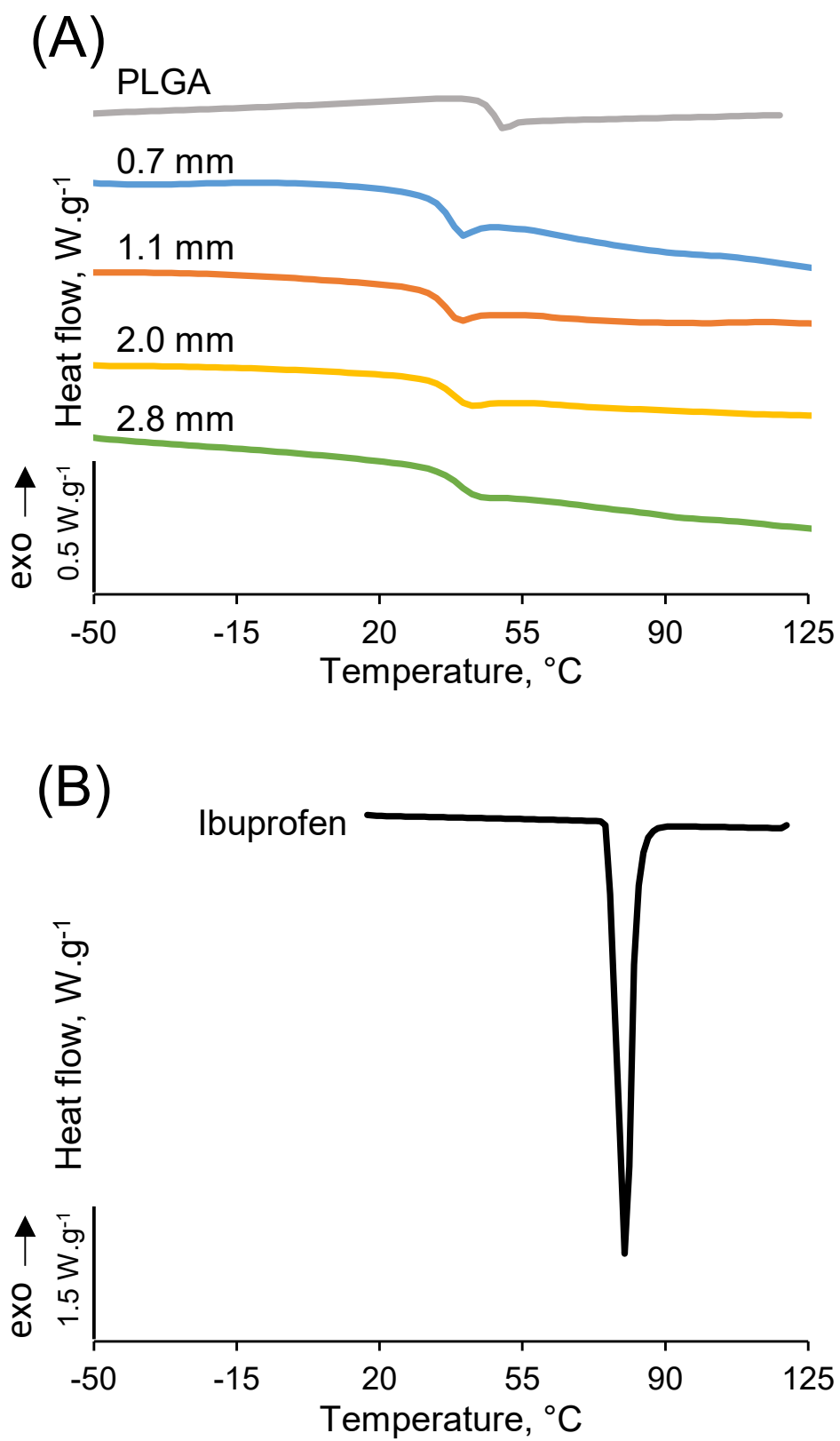


Figure 3

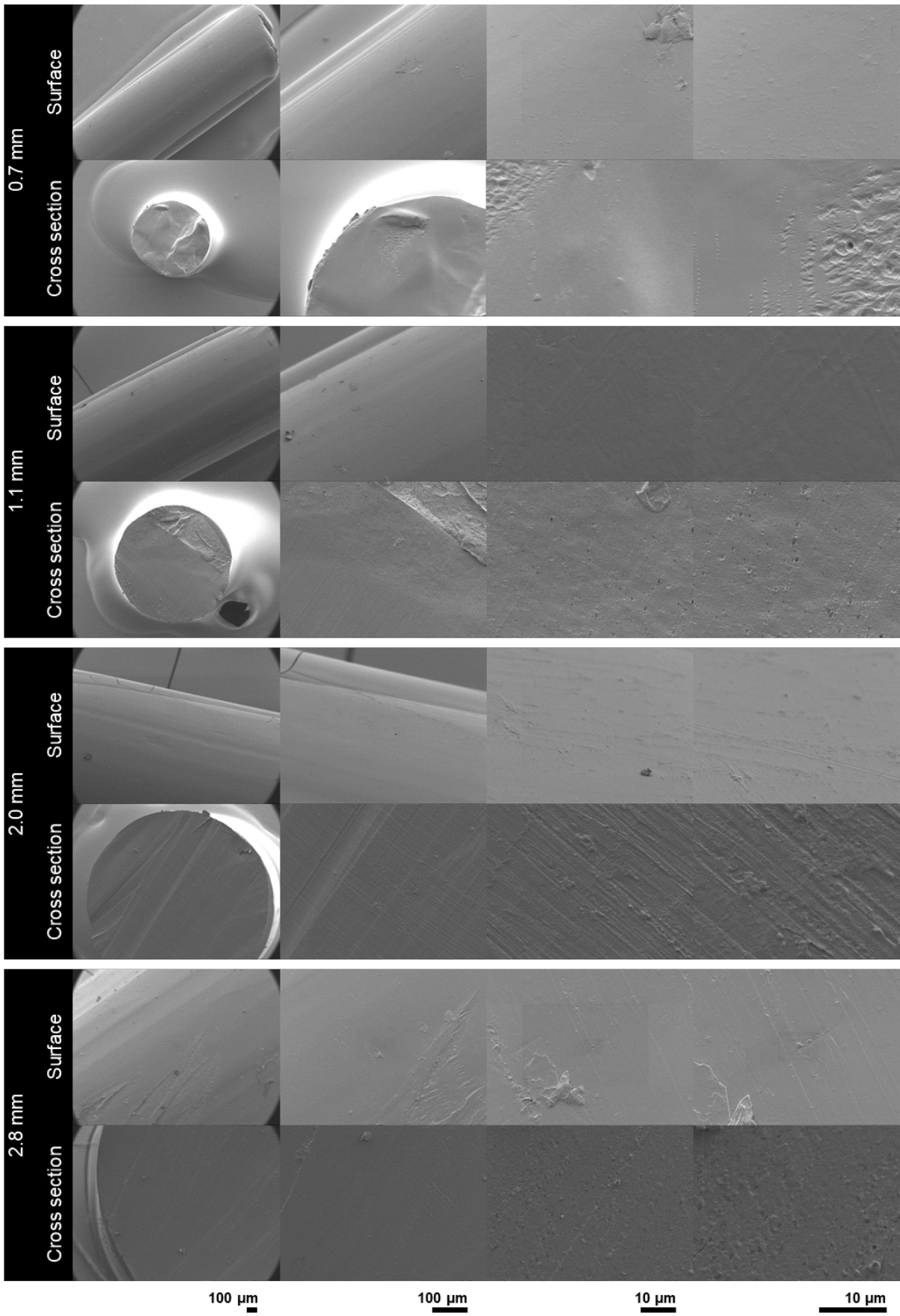


Figure 4

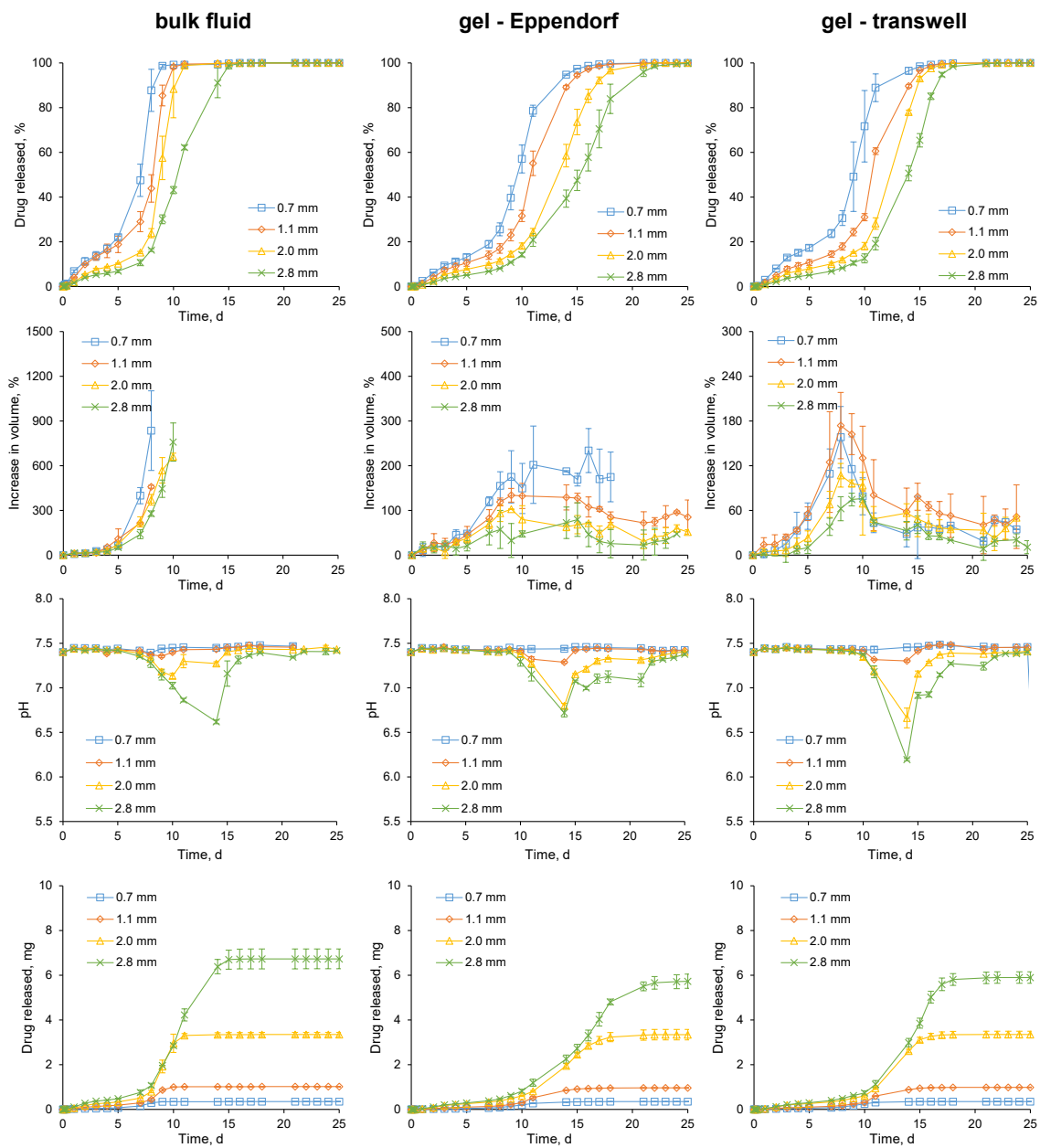


Figure 5

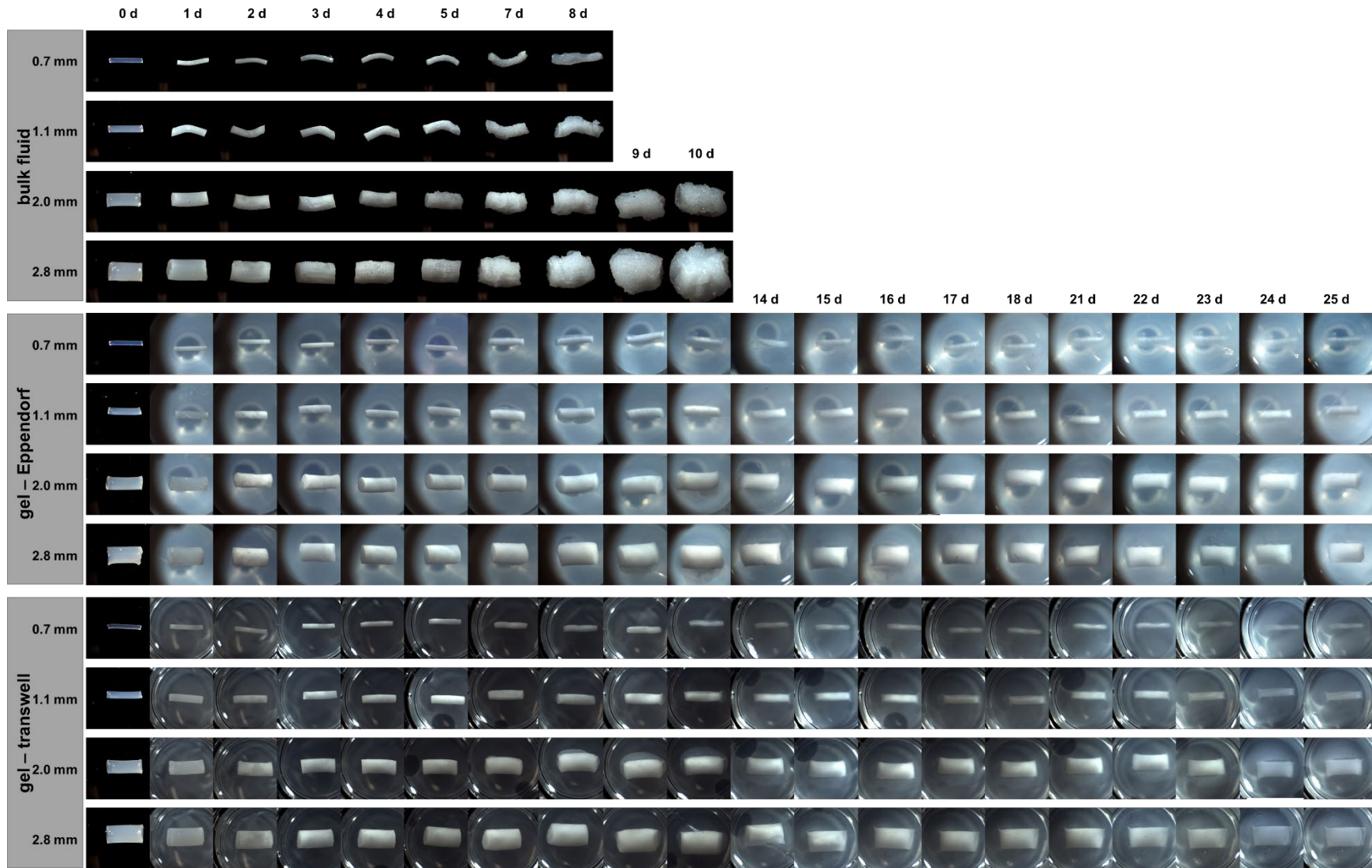


Figure 6

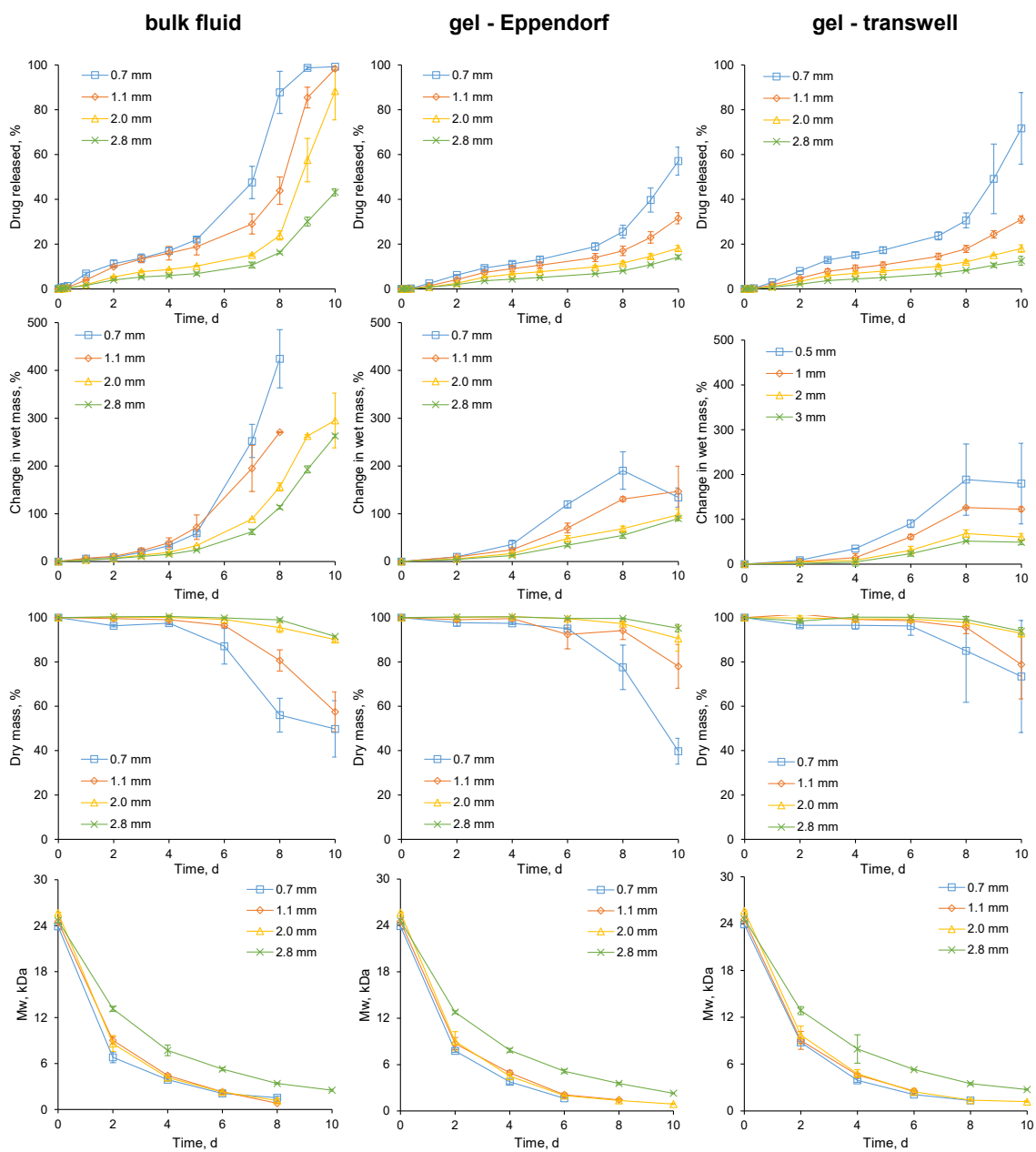


Figure 7

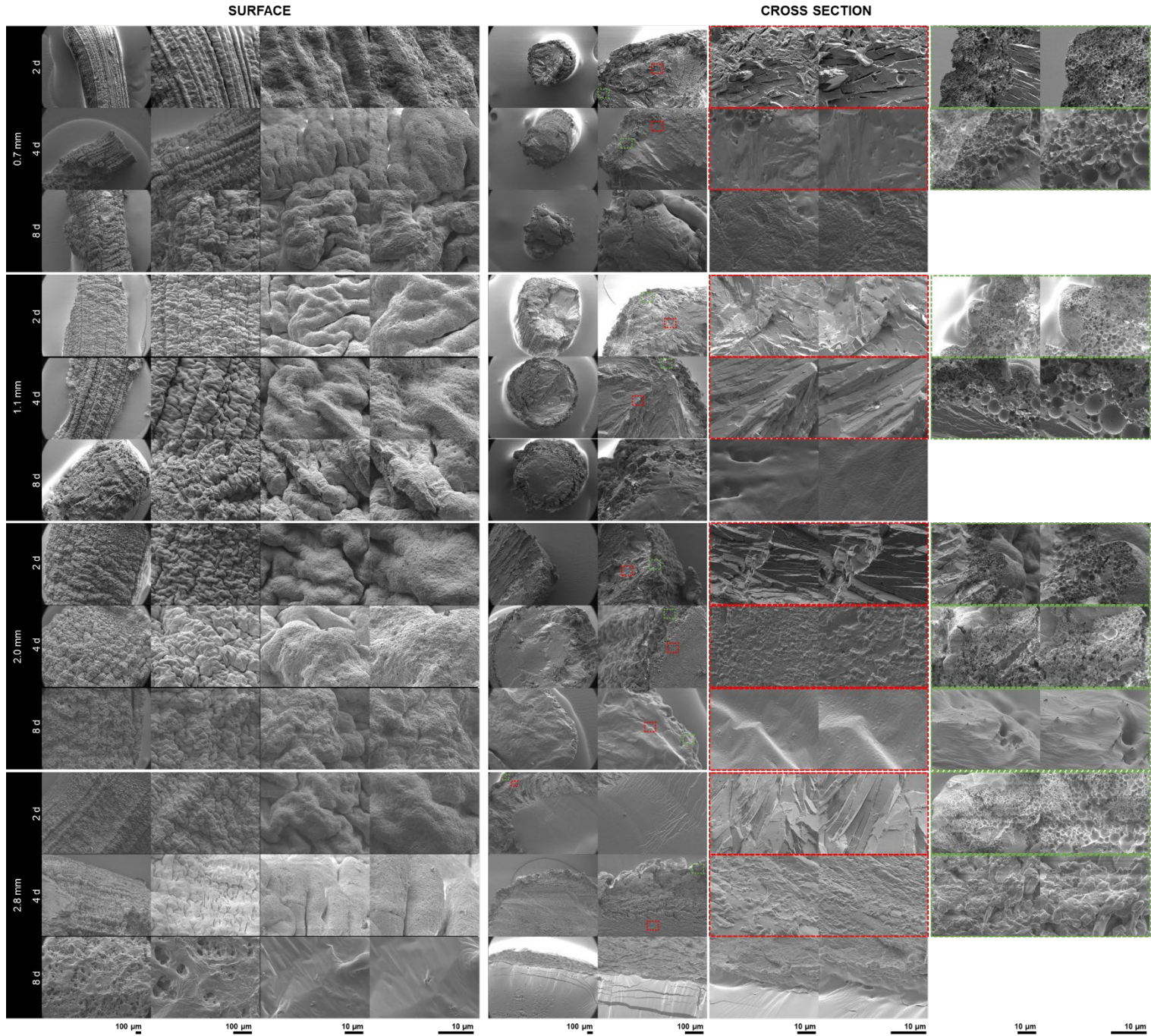


Figure 8